

Studying extreme Arctic sea ice lows with rare event simulation techniques

J. Sauer¹, F. Ragone^{1,2}, F. Massonet¹, G. Zappa³, J. Demaeyer²

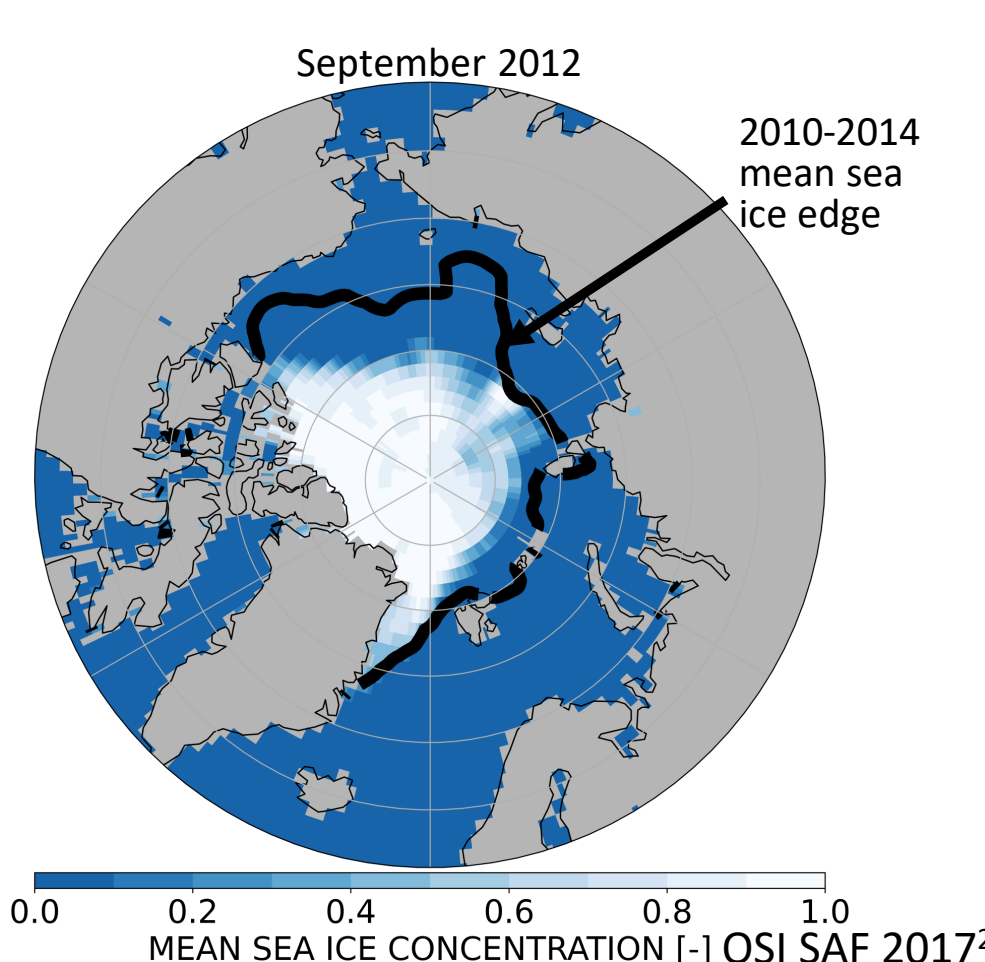
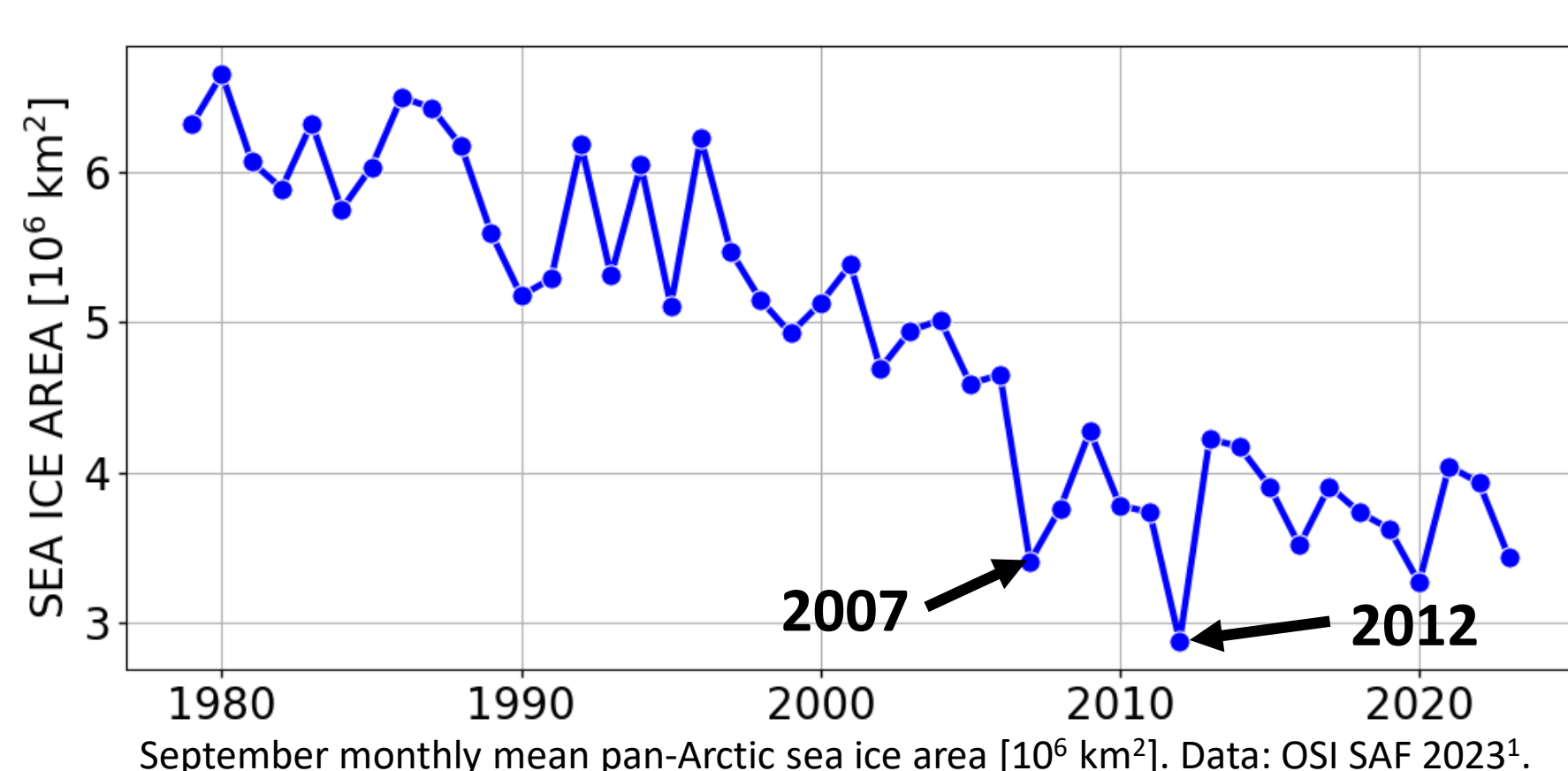
¹Earth and Climate Research Center, Earth and Life Institute, Université catholique de Louvain, Belgium

²Royal Meteorological Institute of Belgium, Brussels, Belgium

³National Research Council of Italy, Institute of Atmospheric Sciences and Climate, Bologna, Italy

jerome.sauer@uclouvain.be

Introduction: Extreme Arctic sea ice lows



Goal: Understanding the physical drivers and predictability of extreme Arctic sea ice lows
→ Preconditioning, sea ice-albedo feedback, oceanic and atmospheric circulations

Problem: Quantitative statistical analyses of **climate extremes** hindered by the **lack of data** in observations and **computationally expensive numerical simulations**

→ Improve the sampling efficiency of **extremes** in climate model simulations with **rare event algorithms**

→ **Genealogical selection algorithm** adapted from Del Moral and Garnier (2005)³; Giardina et al. (2011)⁴ (Ragone et al. 2018⁵; Ragone and Bouchet 2019⁶, 2021⁷): Efficient to study time-persistent extremes

Application of the rare event algorithm to PlaSim-T21-LSG

- 5 x 600 trajectories run from **independent initial conditions taken from control run** (Sauer et al., 2023⁸)
- The algorithm enables to **oversample extreme summer sea lows**, to **compute return times up to more than 10^5 years with a computational cost of order 10^3 years** (Figure 2(a-b)) and to **improve the statistical accuracy of composite maps** compared to the control run (Figure 3)

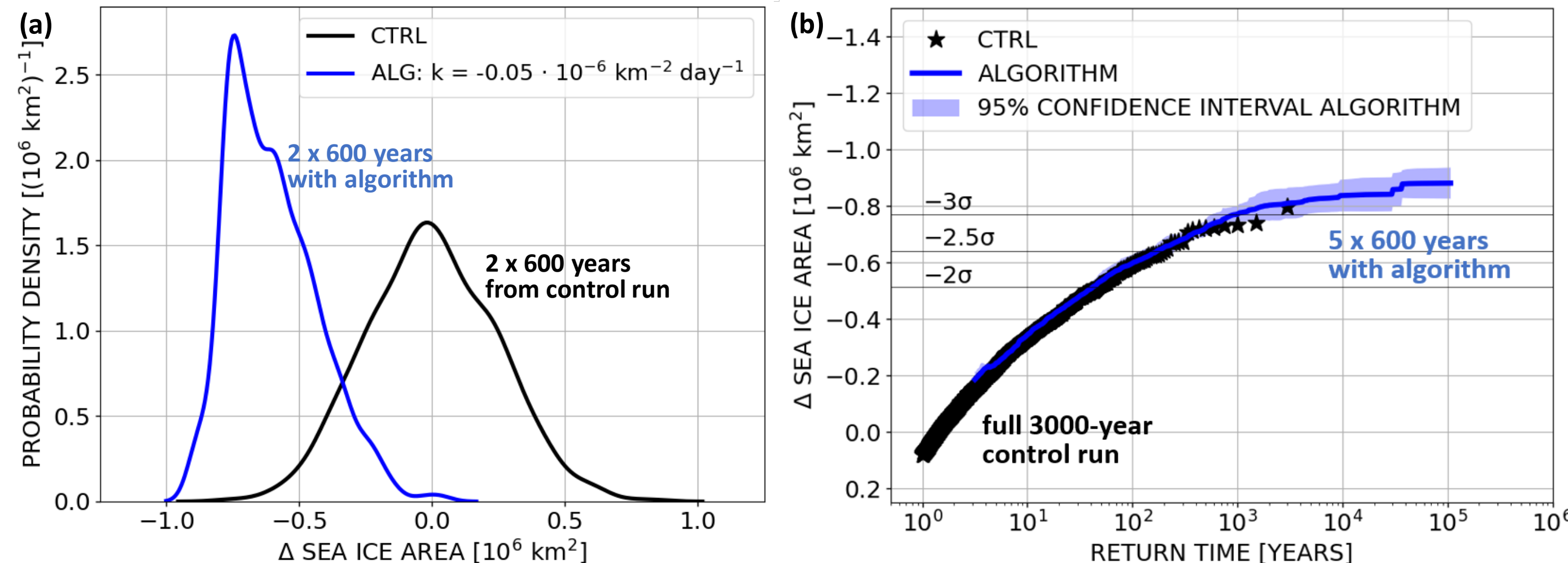


Figure 2: (a) February-September mean pan-Arctic sea ice area anomalies relative to the climatology of the control run for (black) two control ensembles and (blue) two rare event algorithm ensembles. (b) Return times estimated from (black) the control run and (blue) from five ensembles with the rare event algorithm. The blue shading marks the 95% confidence interval.

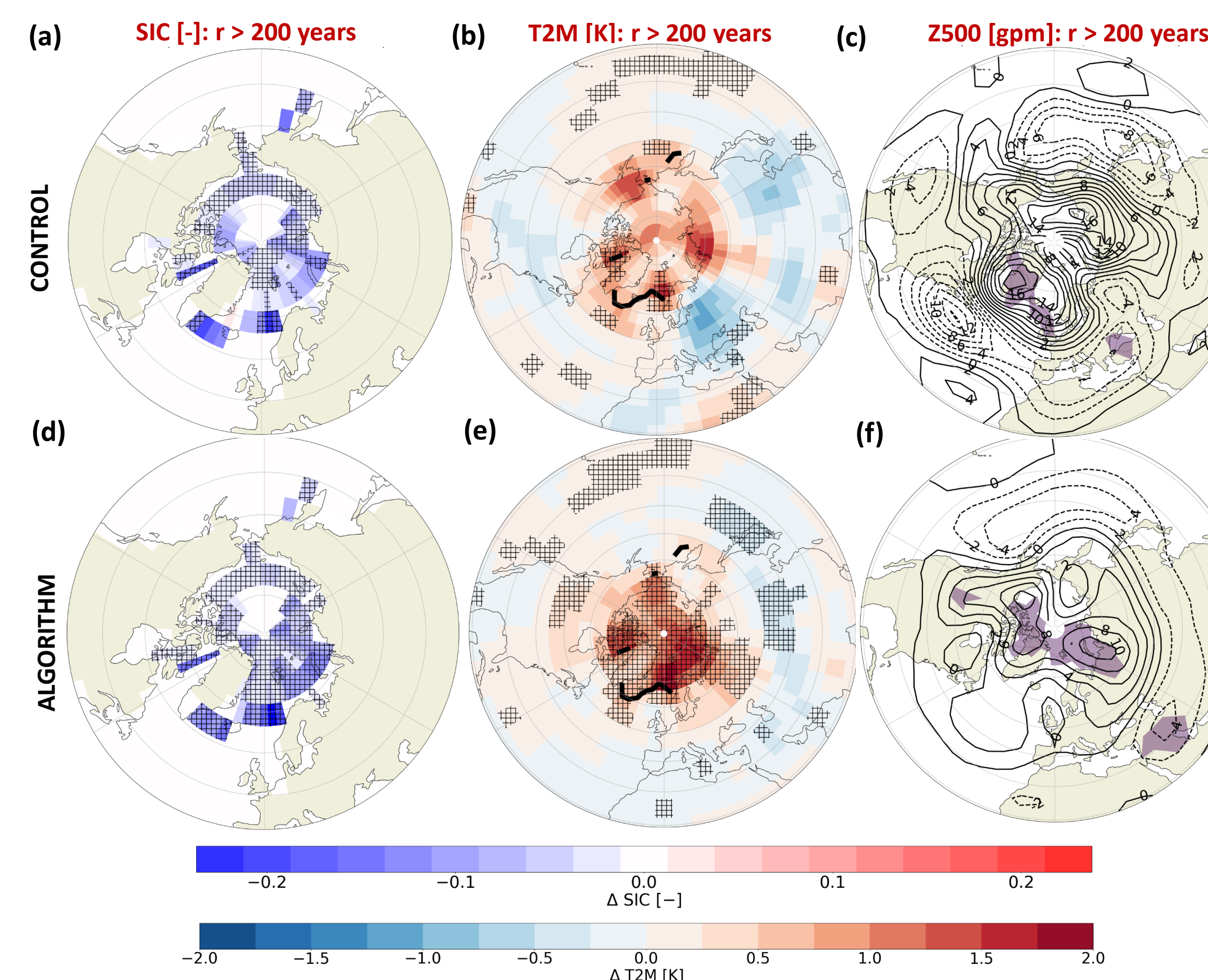


Figure 3: Composite maps: Mean (a,d) sea ice concentration (SIC [-]), (b,e) two metre temperature (T2M [K]) and (c,f) 500 hPa geopotential height (Z500 [gpm]; contour interval 2 gpm) anomalies during seasons of extreme negative pan-Arctic sea ice area anomalies with return times of more than 200 years for (top) the control run and (bottom) the rare event algorithm. All anomalies are averages over the extended summer season from February to September and are estimated relative to the climatology of the control run. (a,b,d,e) Hatching and (c,f) shading denotes statistical significance at the 5% level according to a two-sided t-test. (b,e) The black contour line shows the climatological February-September mean sea ice edge defined as the 15% sea ice concentration contour line.

- Extreme February-September mean Arctic sea ice lows in PlaSim-T21-LSG associated with
 - 1) Winter preconditioning in the sea ice-ocean system
 - 2) Anomalously humid and cloudy Arctic atmosphere throughout late winter and spring
 - 3) Arctic "heatwave" in early summer
 - 4) Sea ice-albedo feedback (Figure 4)

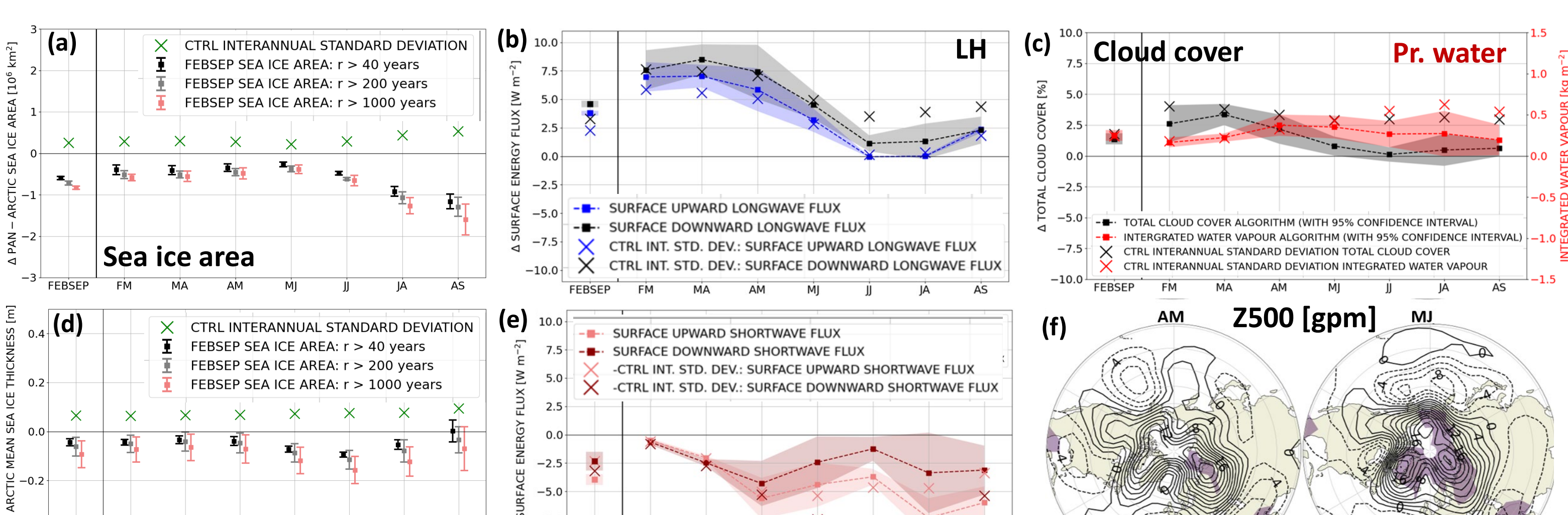


Figure 4: Composites from experiments with the rare event algorithm: (a) Mean pan-Arctic (a) sea ice area [10^6 km^2] and (d) sea ice thickness (m) anomalies during seasons of extreme negative February-September (FEBSEP) mean pan-Arctic sea ice area anomalies with return times of more than (black) 40 years, (gray) 200 years and (red) 1000 years. (b,c) Mean anomalies of domain-averaged quantities (average over all oceanic grid boxes north of 70°N) during extremely low sea ice seasons with return times of more than 200 years. Anomalies of (b) the (blue) upward and (black) downward surface longwave radiative flux [W m^{-2}], (c) the total cloud cover [%] and (red) the integrated water vapour [kg m^{-2}] and (e) the (lightblue) upward and (darkred) downward surface shortwave radiative flux [W m^{-2}]. (b,e) Direction-independent absolute values of the downward and upward radiative fluxes are considered, i.e., a positive (negative) anomaly indicates a radiative flux that is stronger (weaker) in magnitude than the climatology. (f) Composite mean 500 hPa geopotential height (Z500 [gpm]; contour interval 2 gpm) anomalies during seasons of extreme negative pan-Arctic sea ice area anomalies with return times of more than 200 years for April-May (AM) and May-June (MJ) and estimated with the rare event algorithm. Shading and error bars in (a-e) indicate 95% confidence intervals and shading in (f) statistical significance at the 5% level.

Methodology: Rare event algorithm

- **Importance sampling** of trajectories in ensemble simulation with numerical model
 - make trajectories leading to **large anomalies** of a **time-averaged observable** common
 - **better statistics on extreme events** (composites, return times) + **generation of ultra-rare events**
- 1) Consider N trajectories $\{X_n(t)\}$ ($n = 1, 2, \dots, N$), an **observable** $A(\{X_n(t)\})$, a **total simulation time** T_a and a **resampling time** τ_r
- 2) At regular times $t_i = i\tau_r$ ($i = 1, \dots, \frac{T_a}{\tau_r}$), trajectories are **killed** or generate a number of **replicates** depending on the **weights**
- 3) After the simulation: **reconstruction of effective ensemble** based on surviving trajectories
- 4) **Importance sampling formula:** relates probabilities of trajectories between control simulation and simulation with the rare event algorithm

$$P_k(\{X(t)\}_{0 \leq t \leq T_a}) = \frac{e^{k \int_0^{T_a} A(X(t)) dt}}{R} P_0(\{X(t)\}_{0 \leq t \leq T_a})$$

P_k, P_0 : prob. dens. in biased and unbiased statistics
 k, R : biasing parameter and normalization term
 t, T_a : time and simulation length
 $A, \{X_n(t)\}$: observable and model trajectories

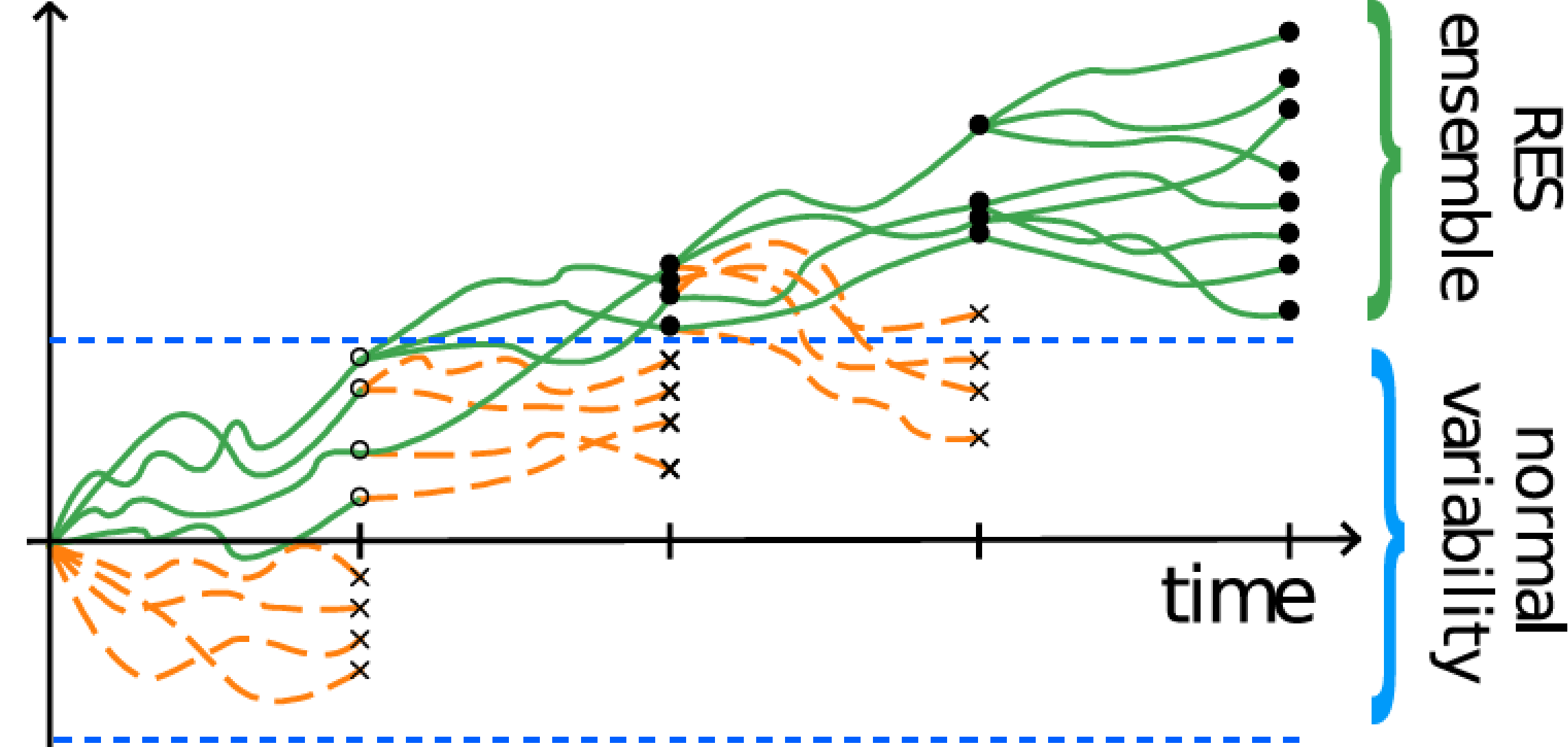


Figure 5: Illustration of the rare event algorithm. Figure from Wouters et al. 2023⁹

Future application of the algorithm to EC-Earth3.3.1

Model version	Resolution	Forcing and initialization
- EC-Earth3.3.1 (Dösscher et al. 2022 ¹⁰) - IFS: T255L91	- NEMO-3.6 including LIM3.6	- Fixed greenhouse gas conditions and solar forcing at year 2000 level - NEMO: ORCA1L75 - Year-2000 NEMO restart files of historical run with EC-Earth3.3.2

Control run:

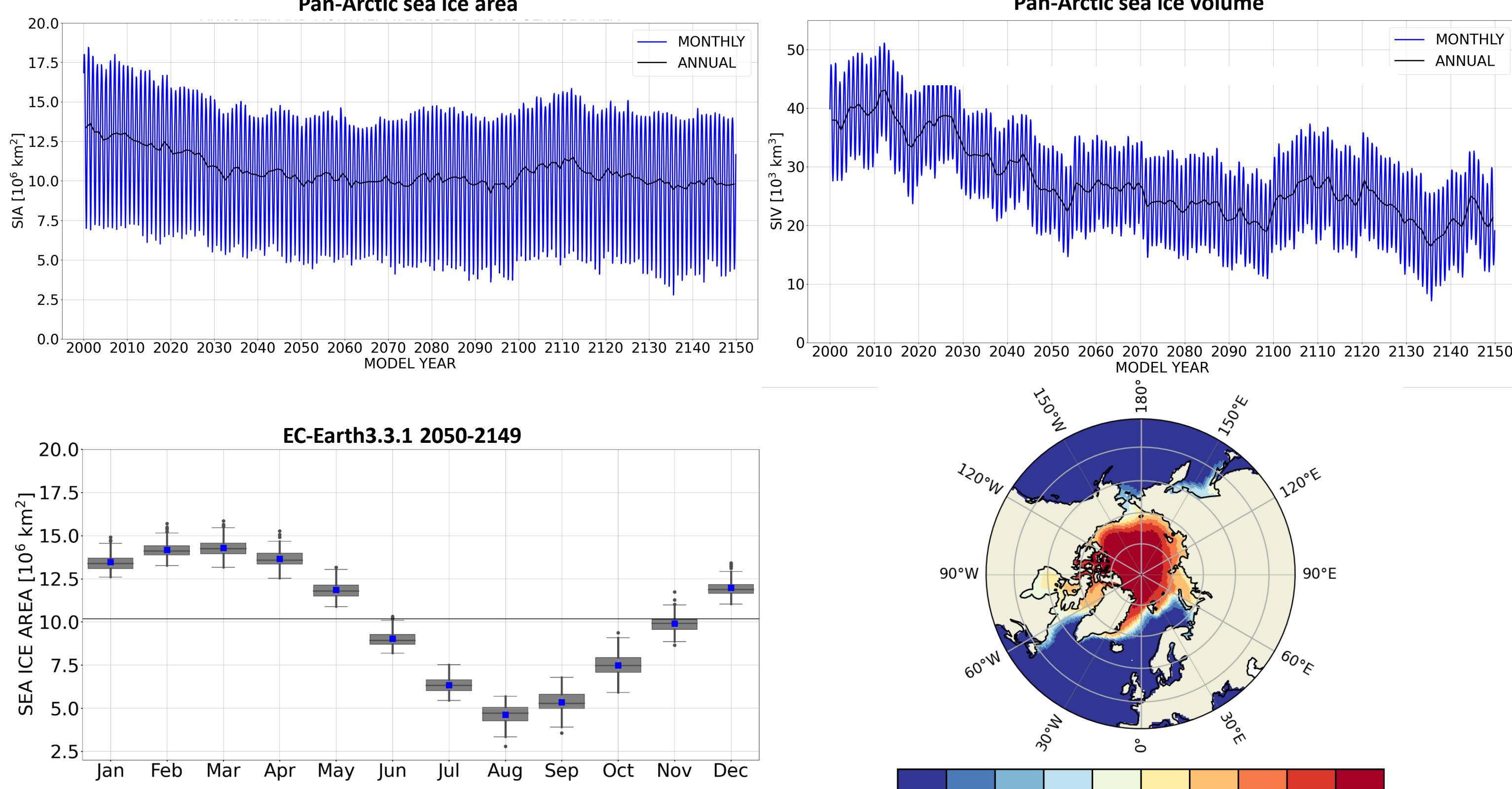


Figure 6: Pan-Arctic sea ice area and sea ice volume and annual mean sea ice concentration field are computed from years 2050-2149.

Possible application with the rare event algorithm:

Start ensemble with the rare event algorithm from initial condition from a year with an extreme Arctic sea ice low:

- What is the probability of observing an extreme sea ice low conditional on that initial state?
- How extreme could the sea ice low have become?
- What are the physical drivers of the extreme sea ice low?

References

- 1) OSI SAF 2023, http://osisaf.met.no/prod/test/ice/index/v2p1/nh/osisaf_nh_sia_daily.nc
- 2) OSI SAF 2017, <http://osisaf.met.no/reprocessed/ice/conc/v2p0>
- 3) Del Moral, P. and J. Garnier, 2005, <https://doi.org/10.1214/105051605000000566>
- 4) Giardina, C., J. Kurchan , V. Lecomte, et al., 2011, <https://doi.org/10.1007/s10955-011-0350-4>
- 5) Ragone, F., J. Wouters and F. Bouchet, 2018, <https://doi.org/10.1073/pnas.1712645115>
- 6) Ragone, F. and F. Bouchet, 2020, <https://doi.org/10.1007/s10955-019-02429-7>
- 7) Ragone, F. and F. Bouchet, 2021, <https://doi.org/10.1029/2020GL091197>
- 8) Sauer, J. et al., 2023, preprint available under <https://doi.org/10.48550/arXiv.2308.09984>
- 9) Wouters, J., R.K.H. Shiemann and L.C. Shaffrey, 2023, <https://doi.org/10.1029/2022MS003537>
- 10) Dösscher, R. et al., 2022, <https://doi.org/10.5194/gmd-15-2973-2022>